On-Chip Optical Nano-Tweezers for Culture-Less Fast Bacterial Viability Assessment

Manon Tardif, Emmanuel Picard, Victor Gaude, Jean-baptiste Jager, David Peyrade, Emmanuel Hadji, Pierre Marcoux

On-Chip Optical Nano-Tweezers for Culture-Less Fast Bacterial Viability Assessment

*Manon Tardif, Emmanuel Picard, Victor Gaude, Jean-Baptiste Jager, David Peyrade, Emmanuel Hadji, and Pierre R. Marcoux**

M. Tardif, E. Picard, J.-B. Jager, E. Hadji Univ. Grenoble Alpes
Grenoble INP CEA
IRIG
Pheliqs SiNaPS Lab
Grenoble F-38000, France
M. Tardif, V. Gaude, D. Peyrade Univ. Grenoble Alpes
CNRS LTM
Grenoble F-38000, France
P.R. Marcoux
Univ. Grenoble Alpes CEA
LETI DTBS LSIV
Grenoble F-38000, France
E-mail: pierre.marcoux@cea.fr

ABSTRACT

Because of antibiotics misuse, the dramatic growth of antibioresistance threatens public health. Tests are indeed culture-based, and require therefore one to two days. This long time-to-result implies the use of large-spectrum antibiotherapies as a first step, in absence of pathogen characterization. Here, a breakthrough approach for a culture-less fast assessment of bacterial response to stress is proposed. It is based on non-destructive on-chip optical tweezing. A laser loads an optical nanobeam cavity whose evanescent part of the resonant field acts as a nano-tweezer for bacteria surrounding the cavity. Once optically trapped, the bacterium-nanobeam cavity interaction induces a shift of the resonance driven by the bacterial cell wall optical index. The analysis of the wavelength shift yields an assessment of viability upon stress at the single-cell scale. As a proof of concept, bacteria are stressed by incur- sion, before optical trapping, at different temperatures (45, 51, and 70 °C). Optical index changes correlate with the degree of thermal stress allowing to sort viable and dead bacteria. With this disruptive diagnosis method, bacterial viability upon stress is probed much faster (typically less than 4 h) than with conventional culture-based enumeration methods (24 h).

1. Introduction

Antibiotic bacterial resistance kills an estimated 700 000 people each year worldwide, and experts predict that this number could rise to 10 million by 2050[1] if counter efforts are not made. Rapid diagnosis could play an essential role in the fight against this alarming phenomenon by prescribing the appropriate antibiotherapy as soon as possible, reducing thus the unnecessary use or misuse of

antibiotics. Clinical microbiology has relied on culture as the standard method for characterizing pathogens over the past century. This process is time-consuming and requires large biomasses.[2] In this context, fast single-cell characterization techniques would be a significant break-through. Optical nano-tweezers have recently appeared as a way to trap bacteria in a nondestructive way[3–10] making this approach a possible key component in future microbiology. Currently, several techniques are used to probe the optical properties of cells[11–16] and more specifically of bacteria. These range from light scattering[17–19] and light transmission monitoring[20,21] to quantitative phase microscopy and immersion refractometry.[12,22–24] Most of them evaluate the average optical Refractive index (RI) of bacteria, or properties in relation to optical index. However, this mean value does not reflect the complex structure and mechanisms of the microorganism be

it at the scale of colony or single-cell. Current interest in this outer part of the bacterium is driven by the need to understand the composition,[25] metabolites,[26] motility,[27] and mechanical properties[28,29] of bacteria. The bacterial cell wall is also widely studied for the identification (specific detection) of bacteria according to their surface composition (immuno-assays).[30,31] Furthermore, as it constitutes the major part of the bacterial biomass, the cell wall is also a good indicator of the effect of antibiotics, as they induce an oxidative stress and a subsequent oxidation of cell wall.[32,33] As a result, the RI of the cell wall can be considered as a key parameter[25,34] to address. Unfortunately, to the best of our knowledge, there is no method to date that permits the easy determination of cell wall RI of living cells. R. E. Marquis proposed in 1973 a method[35] that enables cell wall RI determination in the highly specific case of dead Gram-positive bacteria after complex and denaturing sample preparation (heating, centrifugation, separation). A more recent alternative, based on immersion refractometry,[12,22–24] requires a complex optofluidic imaging system that can simultaneously trap cells and immerse them in a liquid of adjustable RI.

Here we demonstrate the trapping of bacteria in the evanescent field of an optical nanobeam cavity and the real-time dynamic analysis of their physical properties. The field of these optical cavities and the change of resonance frequency induced by an index change within its evanescent field were previously characterized through the use of SNOM (Scanning Near-fi Optical Microscopy).[36,37] This resonance shift was further studied through the trapping of beads having a given RI.[38] After all those characterizations of the microresonator and its evanescent field, complex biological microparticles such as bacteria were trapped.[6,7] This label-free approach makes it possible to probe solely the RI of the bacterium cell wall ($n$wall) and therefore monitor how a stress can affect this index in trapping conditions. Bacteria are thus compared before and after thermal stress and the different optical signatures are commensurate with the stress intensity. This shows that nwall, as a property of the interface between the external medium and the bacterium cytoplasm, reflects the state of a bacterium (stressed, alive, dead). This new bacteria assessment approach is finally corroborated by standard culture-based methods (counting of bacteria on Petri dishes). The results evidence that on-chip monitoring of the near-field interaction with an optical resonator-based integrated device may strongly reduce the time needed to assess bacterial state and test the response of bacteria to an external stress.

2. Results and discussion

2.1. The interaction between Nanocavity and bacterium cell wall

Recent experiments have shown that photonic crystal-based structures can be used to trap and manipulate polystyrene beads[10,30–33,38–41] and, later on, to trap living material like bacteria.[5–10] Based on these preliminary results, we developed a two-laser setup to simultaneously trap a single object in the near field (<80 nm) of a nanobeam microcavity and probe its RI in the vicinity of the microresonator surface. In our experiment, these two optical sources are infrared tunable lasers

connected to an injection fiber by a 1.55 μm 2 × 1 fiber-optic coupler. Light is injected into the optical structure (microcavity) at its resonant wavelength in an aqueous external medium (_H2O), creating an intense and confined electromagnetic field (EMF). The evanescent part of this EMF is delocalized around the microcavity and allows the trapping of micron-sized objects by optical gradient forces. The resonator is immersed in a suspension of bacteria in deionized water within a static fluidic system. While the first source injects the resonant wavelength beam into the water-enclosed cavity (λH2O) to trap bacteria, the second scans around this wavelength (λi···λf) in order to extract the resonant wavelength of the cavity in the presence of the trapped bacteria (λbact). Indeed, when a bacterium starts to interact with the EMF of the microcavity, the successful trapping leads to a redshift of the resonance (Figure 1a). From this, the resonance shift Dλ=λbact- λH2O that appears in the presence of a trapped bacterium is calculated. The proof-of-concept bacterium used as a model in this paper is Escherichia coli, an extremely widespread peritrichous, gram-negative, rod-shaped (1 × 2 μm size) bacterium (Figure 1b). Thanks to a dual-mode monitoring that combines microscopy imaging with transmission monitoring through the microcavity, the trapped bacteria can be seen during the whole experiment (Figure S2,Supporting Information).

All bacteria trapping is performed in water, using a single nanobeam microcavity with a quality factor of about 2800 (Figure 1c). The dispersion of the RI was not considered in the visible/infrared spectral ranges.

In order to correlate the resonant wavelength shift to the bacterium properties, FDTD (Finite-Difference Time-Domain)[42] calculations were performed to get a fine understanding of bacterium – cavity near-field interaction and pinpoint, at wavelength scale, the exact part of the bacterium that interacts with the evanescent part of the field during trapping (Figure 2a). First, the cavity was modeled in a homogeneous medium of index 1.380 (in agreement with the RI values of bacteria measured in the work of Bateman et al.[43] and P. Y. Liu[12,22,24]). The resonance shift of the cavity upon a media change to water (n =1.330) was found to be 4.7 nm (as shown by the horizontal black line in Figure 2b). Then, an E. coli

type object with a RI of 1.380 was modeled at different altitudes (i.e., the distances between the bacterium and the cavity center), immersed in water. The length variations of the model cell were neglected (when a bacterium is dividing). The typical duration of a single measurement of the shift resonance is indeed about 10 s, that is, several orders of magnitude faster than the shortest bacterial doubling times (1200 to 1500 s). The resonance wavelength shift Δλ (bact H2O __ = _ −_) of the cavity was calculated according to the vertical position of the cell in a range of 0–100 nm from the optical structure. The lateral x-y displacements of the model cell were neglected, as previous studies have highlighted that the amplitude of bacterial movements is significantly reduced when it is trapped. We also previously evidenced that the small resonance shifts due to bacterial motility and Brownian motion under trapping are much smaller than the Δλ parameter presented in this paper.[6,7]

The cavity-bacterium interaction decreases when the distance between them increases (as shown by the green curve on Figure 2b). The resonance wavelength shifts by 2.2 nm between 0 and 80 nm (bacterium altitude). Beyond this distance, the trap no longer detects the presence of the bacterium and the resonant wavelength returns to that of a cavity enclosed in a water medium. This 80 nm upper limit for the bacterium altitude is consistent with the decrease of the evanescent field plotted in Figure 2b (blue curve). As a conclusion, we can assume that, under trapping, only the first 80 nm of bacterium matter interacts with the EMF of the microcavity. In the case of E. coli (a Gram-negative species),[44,45] this 80 nm range corresponds to almost the entire thickness of the bacterial cell wall. This part of the bacterium is more specifically composed of an outer membrane (7.5–10 nm thick), a periplasmic space (30–70 nm) with peptidoglycan (5–10 nm) and a plasma membrane (7.5 nm)[45,46] (Figure 2a).

Since Δλ is dependent on the bacterium altitude above the cavity, we build an abacus using 3D FDTD simulation for a number of cavity-bacterium distances to pinpoint the link between Δλ and the RI of the trapped bacterium. The result is shown in Figure 2c. Thus, after experimentally measuring the resonant wavelength shift Δλ, we deduce the bacterium RI from the abacus. For E. coli that are not thermally stressed, the measured shift is Δλ1=0.171 • } 0.043 nm (measured at 25 °C on American Type

Culture Collection (ATCC) 11 775 strain, on 58 distinct bacteria from independent cultures), which we highlighted as a dashed line in Figure 2c. In the 0–50 nm distance range, the corresponding RI lays between 1.334 and 1.347 (Table S1, Supporting Information). Finally, although the experimental distance between the bacterium and the microcavity remains unknown, this method yields a cell wall RI of 1.340 with a resolution of 10−2 refractive index unit. These results are in good agreement with the work of R. E. Marquis on Grampositive bacteria,[35] which has a thick membrane consisting only of peptidoglycan. This author used immersion refractometry to demonstrate that cell wall RI is lower than the average index of bacteria, and is between 1.348 and 1.382. As these values are close to our modeling value of 50 nm (cavity-bacterium distance), we will arbitrarily select this 50 nm distance for this study, excluding the contact as the trapping is reversible. At this altitude, we can conclude that only the outer membrane, the periplasmic space and the peptidoglycan of E. coli are probed. The index presented here is therefore an average RI cell wall value. Compared to the previously presented techniques used for bacteria RI sensing, this optical method based on the trapping on a micro-resonator has the advantages of a single-cell study, reproducibility of RI determination, and sub-micron local probing. On the opposite, it has the major drawback of not yielding an absolute RI value, as the exact distance between cell and cavity is not known.

2.2. Study of the Effect of Thermal Stress

Now that we have outlined the trap (nanocavity) – bacterium cell wall interaction, we would like to evidence if a physical or chemical damage of the cell wall could be probed by a change in this interaction. We choose to study the effect of thermal stress, which causes damage to the bacterial cell wall.[47–50]. Experiments are conducted at key temperatures[47] of 37 °C (optimum culture temperature), 45 °C (moderate heat stress), and finally 51 °C (high stress) and 70 °C (pasteurization). E. coli bacteria are subjected to these temperatures and then analyzed by trapping at room temperature. Average $\Delta\lambda$ was measured at 25 °C as a function of stress time. The procedure is detailed in the Experimental Section and the results are shown in Figure 3a. In this figure, the evolution of the resonant wavelength of the

cavity is plotted as a function of the heating time. The shift of the trapped bacteria RI compared to a non-stressed bacterium (i.e., a bacterium that has not been subjected to thermal stress) is also shown (Δn). At temperatures above 37 °C, three stages become apparent: the Δλ increases (as does the RI of the trapped bacterium cell wall), then decreases, and finally stabilizes. We also observe that the cell wall RI increases faster at higher temperatures.

The maximum shift in resonance is about 0.300 nm, which corresponds to a probed RI of 1.360 (which corresponds to Δn = 0.012). This maximum is reached after 12 min at 70 °C, 50 min at 51 °C, and 140 min at 45 °C. Measurements are stable during the 210-min experiment at 37 °C, which allows us to use the latter as a reference. The experiment was carried out over 250 min at 37 °C and 45 °C but only 130 min at 51 °C and 30 min at 70 °C. Although the bacterial cell wall is still visible for the two highest temperatures, it was impossible to trap bacteria after these periods of heating.

The results shown in Figure 3a demonstrate that thermal stress has a direct influence on the RI of the bacterial cell wall. The literature shows that heat stress in E. coli is initially reflected by a modification of the cell wall composition[48–50] due to oxidative stress.[51,52] The state of the cells then changes from viable and culturable to viable but non-culturable (VBNC). Finally, a mechanism of lysis of the damaged cells deteriorates the integrity of the cell wall. In Figure 3a, we interpret the three steps that we observe as follows: the increase in RI corresponds to this mechanism of cell wall oxidation, while its decrease corresponds to a mechanism of destruction (cell wall porosity) leading eventually to death (loss of cell wall integrity). Further single-cell characterization, such as Raman microspectroscopy for chemical modifications of bacteria,[53] and fluorescence microscopy with live/dead staining for the visualization of (non)permeable cells,[54] should strengthen this interpretation in the future. We propose two hypotheses to explain the impossibility of trapping bacteria after 130 min at 51 °C and 30 min at 70 °C. Firstly, the bacterial cell wall RI may fall too low to allow cell trapping; the gradient optical forces are a function of the RI contrast between the trapped object and the suspension medium. The second possibility is that the cell lysis process has already begun. The variability in the Δλ measurements found

on the black curve (Figure 3a) at 37 °C is approximately 0.042 • } 0.027 nm (minimum-maximum range • } mean standard deviation). This phenomenon was also observed at t = 0 min for all experimental curves, and required normalization. This variability is mainly due to extremely local variations in temperature related to the confinement and concentration of light in the structure. For more precision, other experimental measurements were conducted to evaluate the variability of the measurement of $\Delta\lambda$ at trapping laser power (Figure S3, Supporting Information). This variability is estimated at approximately 0.045 nm and appears to be independent of the temperature of the sample (trapping optical structure). As an example, the mean value and the standard deviation of the measurements (10 to 20 independent bacteria per data point) for a fixed temperature (51 °C) are shown in Figure S4, Supporting Information.

2.3. Comparison with the Standard Culture-Based Methods

In order to evaluate the reliability of our results on bacterial stress monitoring using optical resonators, we confronted them with measurements commonly used in microbiology to determine the effect of temperature on bacteria based on their culturability. The Encyclopedia of Food Microbiology[55] describes a method to quantify the reduction of viability within a population of thermally stressed bacteria, based on counting of CFU on Petri dishes. At regular intervals, samples were taken from bacteria subjected to thermal stresses at the temperatures under study (45, 51, and 70 °C). They were then cultured on agar and the number of microorganisms that survived the heat stress was determined through counting of colonies after a 24 h incubation at 37 °C. For further details on the protocol used refer to the Experimental Section. These results are used to calculate the proportion of culturable bacteria in the sample at any moment. The curves of the Figure 3b indicate the proportion of culturable bacteria in the samples heated at 37, 45, 51, and 70 °C. A decline occurs in the proportion of culturable bacteria in the sample as the stress time increases. The higher the temperature, the faster the population decreases.

The vertical lines indicate the moments when the maximum of each curve ($\Delta\lambda$ and RI) is reached in Figure 3a. When we compare these moments with the curves of Figure 3b, we realize that they always correspond to a three-decade decay (<0.1 % of survivors), whatever the heating temperature. The curve at 37 °C is dotted because it is deduced from the other three curves. The observed diminution at 37 °C is due to the stress suffered by the bacteria in a hypotonic medium, and corresponds to the reference conditions with no heat stress. Experimentally, a good correlation is observed between these two techniques, that is, the single-cell optical characterization (Figure 3a) and the standard culture-based measurement of survivors within a large population (Figure 3b). The peaks of the curves in Figure 3a give us relevant information about the population of culturable bacteria in our sample, since they occur systematically when a maximum of 0.1 % of culturable bacteria remains.

It is important to underline the quantity and quality of the information provided by the optical method. While the classical method of microbiology gives us a binary result (culturable/ non-culturable), the optical method developed in this study allows a detailed analysis of how the state of a bacterium evolves, at a single-cell scale. The information that can be extracted from these intermediate states could lead to a better understanding of bacterial viability, regardless of their cultivability. Moreover, this study highlights an evolution in the state of trapped bacteria that is linked to an external parameter of the cavity. This demonstrates that the act of trapping a bacterium does not cause any damage that leads to its death.

3. Conclusion

This paper demonstrates that optical micro-resonators are key devices to probe the RI of trapped *E. coli* bacteria. The interaction between the trap and the bacterium allows the close inspection of Gram-negative cell wall properties. Similar investigation on Gram-positive bacteria should consolidate these results in a near future. We believe that these results have considerable potential, as this optical method requires very little time and consumables compared to the usual culture- based methods. While the proposed method is conducted in real-time along with bacterial heating and solely requires an optical structure, the conventional

method requirestime-consuming dilution, plate streaking, incubation, and bacterial counting. Moreover, micro-resonator-based devices highlight single-cell variability at the bacterial colony scale, unlike mean population studies. Thus, it opens new perspectives of measuring distributions of phenotypes on a population that faces a stress. This optical method could lead to a better understanding of bacterial viability and VBNC state. Compared with standard culture-based techniques, the proposed methodology shows how the measurement of local optical properties provides crucial insights for bacterial viability. This label-free method is economical in terms of time and consumables and can be extended to any Gram-type bacteria. In the future, the monitoring of finer variation in the state of bacteria in response to other external oxidizing agents—such as antibiotics—will be envisaged.

4. Experimental Section

Optofluidic Chip: The optical microcavities were etched on an silicon on insulator chip of 250 nm/2 μm/700 μm. They were designed to resonate at a wavelength of approximately 1.5 μm with a quality factor of 2800. These parameters were adapted for the trapping of E. coli. A protein treatment was applied to the optical chip to avoid non-specific adhesion of the bacteria to its surface. The chip was immersed in a 5 % solution of bovine serum albumin for 5 min then rinsed and dried. A polydimethylsiloxane pool of 100 μm thickness was deposited above these optical structures. A drop of water with bacteria (≈1 μL) was then placed in the pool and covered with a thin layer of glass (160 μm thick) to avoid evaporation.

Experimental Set-Up: The infrared light was injected directly by the cleaved face of the optical chip into the optical structure by an optical fiber. The injected power required to trap bacteria in the microcavities is between 6 and 16 mW (at exit point of the laser). This corresponds to a power in the trap of around μW for a trap of approximately pN. Since the polarization of the injected light was a key parameter for the optical structures, only polarization-maintaining fibers were used and Lefebvre's loops permit the adjustment of polarization between the source and the structure. The optofluidic chip was monitored in two ways. The first consists of a microscopy column located above the chip which records in real-time up to 30

images per second of the area around the cavity. The second was the use of a photon/electron converter detector which records the optical signal transmitted by themicrocavity in real-time.

Sample Preparation: E. coli strains (ATCC 11775) were obtained from KWIK-STIK lyophilized reference strains (Microbiologics, St. Cloud, MN). They were grown on an agar medium (Columbia sheep blood agar or Trypcase soy agar, bioMérieux). After 24 h of incubation (37 °C), a suspension of 3 McF (Densimat, BioMérieux) was prepared in an API Suspension medium (bioMérieux). This corresponds to a bacterial concentration of 2.109 CFU mL−1. They were then diluted by a factor of 10 in a solution of deionized water previously filtered at 0.2 μm, then incubated at studied temperature (37 °C/45 °C/51 °C/ 70 °C). Samples were collected from this preparation every 15 to 20 min to study the state of bacteria using the two methods described in this article.

Experimental Procedure for the Optical Method: A volume of 50 mL of bacterial suspension at 3 McF was subjected to a given temperature (37 °C/45 °C/51 °C/70 °C) for 3 h. Every 15 to 20 min, 1 mL of bacterial suspension was collected and deposited (≈1 μL) in the optofluidic chip and analyzed at 25 °C. Between 10 and 20 bacterial trappings were carried out during each of these periods. The bacterium was released (i.e., the laser was turned off) between each trapping, thus allowing a different bacterium to be trapped each time.

Experimental Procedure for the Microbiology Method: A volume of 5 mL at 0.5 McF was first diluted in 45 mL, then divided into 10 tubes of 5 mL. The dilution liquids (deionized water filtered at 0.2 μm) had been previously left at the heating temperature for several hours. Every 15 min, a tube was removed and 100 μL volume of its contents was distributed on Petri dishes after dilution (if necessary). The dishes were then incubated for 24 h at 37 °C. A manual count was then performed and the proportion of culturable bacteria was evaluated.

Calculation of the Proportion of Culturable Bacteria in the Sample:DT is the decimal reduction time[55] at T °C (t is duration of exposure to thermal stress, N0 and N are the initial and final numbers of microorganisms):D tNNTlog10 (1)

This parameter denotes the time required to reduce the number of bacteria by a factor of 10 at a given temperature. In the case, the DT-values are as follows: D45 = 39.5 min, D51 = 17.3 min, and D70 = 1.25 min. The information revealed by this decimal reduction time was that the proportion of culturable bacteria in the sample was reduced to 10% after DT min and 1% after 2 × DT min at temperature T °C. The decrease in the bacterial population in the sample during stress time is shown in Figure 3b for each temperature. The decrease in the bacterial population at 37 °C was not measured but was calculated from other DTmeasurements. For this purpose, the parameter z defined as follows is calculated:[55]z T T DT DT–log (/)2 1 10 1 2= (2)

The z-value is defined as the required increase in temperature to reduce the DT-value by a factor of 10. Here, it is defined from two DT-values at distinct temperatures (T1 and T2) and in the case, it was calculated from the slope of the curve representing the DT-values as a function of the temperature for a minimum of three measurements. The measured z-value in the experimental conditions is 16.7 °C. From this, the authors were able to calculate any DT-value and hence the calculation of the bacterial population decrease according to the following: N(t)=N0.10−t/Dx (3)

This decrease in the number of bacteria in the sample exposed to 37 °C (D37 = 119 min) was linked to the stress induced by the non-nutrient and deionized environment in which the bacteria were kept during the experiment (osmotic stress in a hypotonic environment). It is, however, conducted at an optimum temperature which can distort this curve. This is, in anyway, the most favorable curve that can be obtained. These trapping conditions (deionized water for bacterial suspension) were chosen to avoid the adhesion of bacteria to the surface of the sample (optical structures), which occurs frequently when working with bacteria dispersed in a nutrient medium.

***Optical Indices in Infrared and Visible Range*:** FDTD simulation was performed with the RSoft Fullwave software. It was used to calculate the resonant wavelength of the microcavity as a function of the RI of the external medium. These index values are valid at 1.5 μm—the value of the resonant wavelength of the microcavity. In parallel, different media of index between 1.330 and 1.368 were created using various

dilutions of salts (NaCl from 0 %*w*/*w* to 20 %*w*/*w*). The indices of these media were measured using a refractometer at 589 nm. They were then deposited one by one in the optofluidic chip to determine the resonant wavelength of the cavity in these different media. These results are shown in Figure S5, Supporting Information (black curve for simulation (at 1.5 μm), grey stars for experiments (at 589 nm)).

Acknowledgements

The authors thank R. Therisod and R. Houdré (EPFL-Switzerland) for the fruitful discussions they had together. They also acknowledge the technical group of the "Plateforme Technologique Amont" (Grenoble, FRANCE) for their help with nanofabrication. M.T. and E.P. designed and conducted all the experiments. J.-B.J. and V.G. carried out the photonic structures nanofabrication. M.T. and P.R.M. prepared the bacterial samples and conducted all microbiological experiments. M.T., D.P., and E.H. designed the study and wrote the manuscript. All authors discussed the experiments, read and approved the manuscript.

Conflict of Interest

The authors declare no conflict of interest.

Data Availability Statement

The data that supports the findings of this study are available in the supplementary material of this article.

Keywords

nanophotonic tweezers, nanoscale optical sensing, optical trapping, single-cell characterization., viability assessment

References

[1] C. Willyard, *Nature* **2017**, *543*, 15.
[2] A. Belkum, G. Durand, M. Peyret, S. Chatellier, G. Zambardi,
J. Schrenzel, D. Shortridge, A. Engelhardt, W. M. Dunne, *Ann. Lab. Med.* **2013**, *33*, 14.
[3] A. Ashkin, J. M. Dziedzic, *Science* **1987**, *235*, 1517.
[4] S. M. Block, *Nature* **1992**, *360*, 493.
[5] T. Leest, J. Caro, *Lab Chip* **2013**, *13*, 4358.
[6] M. Tardif, J.-B. Jager, P. R. Marcoux, K. Uchiyamada, E. Picard, E. Hadji, D. Peyrade, *Appl. Phys. Lett.* **2016**, *109*, 133510.
[7] R. Therisod, M. Tardif, P. R. Marcoux, E. Picard, J. B. Jager, E. Hadji, D. Peyrade, R. Houdré, *Appl. Phys. Lett.* **2018**, *113*, 111101.
[8] G. Pitruzzello, D. Conteduca, T. F. Krauss, *Nanophotonics* **2020**, *9*,4447.
[9] D. Conteduca, G. Brunetti, F. Dell'Olio, M. N. Armenise,T. F. Krauss, C. Ciminelli, *Biomed. Opt. Express* **2019**, *10*, 3463.
[10] D. Yang, B. Duan, X. Liu, A. Wang, X. Li, Y. Ji, *Micromachines* **2020**,*11*, 72.
[11] L. K. Chin, A. Q. Liu, C. S. Lim, X. M. Zhang, J. H. Ng, J. Z. Hao, S. Takahashi, *Appl. Phys. Lett.* **2007**, *91*, 243901.
[12] P. Y. Liu, L. K. Chin, W. Ser, H. F. Chen, C.-M. Hsieh, C.-H. Lee, K.-B. Sung, T. C. Ayi, P. H. Yap, B. Liedberg, K. Wang, T. Bourouina, Y. Leprince-Wang, *Lab Chip* **2016**, *16*, 634.
[13] P. Y. Liu, *Thesis*, Université Paris-Est, Paris, France **2016**.
[14] B. Vinoth, X.-J. Lai, Y.-C. Lin, H.-Y. Tu, C.-J. Cheng, *Sci. Rep.* **2018**, *8*, 5943.
[15] F. Merola, P. Memmolo, L. Miccio, R. Savoia, M. Mugnano, A. Fontana, G. D'Ippolito, A. Sardo, A. Iolascon, A. Gambale, P. Ferraro, *Light: Sci. Appl.* **2017**, *6*, e16241.
[16] M. M. Villone, P. Memmolo, F. Merola, M. Mugnano, L. Miccio, P. L. Maffettone, P. Ferraro, *Lab Chip* **2018**, *18*, 126.
[17] P. R. Marcoux, M. Dupoy, A. Cuer, J.-L. Kodja, A. Lefebvre, F. Licari, R. Louvet, A. Narassiguin, F. Mallard, *Appl. Microbiol. Biotechnol.* **2014**, *98*, 2243.
[18] V. Genuer, O. Gal, J. Méteau, P. Marcoux, E. Schultz, É. Lacot, M. Maurin, J.-M. Dinten, *Proc. SPIE 9698, Advanced Biomedical and Clinical Diagnostic and Surgical Guidance Systems XIV*, Vol. *9698*,
SPIE, Bellingham, Washington **2016**, p. 96980A.
[19] S. A. Strola, P. R. Marcoux, E. Schultz, R. Perenon, A.-C. Simon,I. Espagnon, C. P. Allier, J.-M. Dinten, *Proc. SPIE 8939, Biomedical Vibrational Spectroscopy VI: Advances in Research and Industry* **2014**,p. 893905.

[20] A. Katz, A. Alimova, M. Xu, P. Gottlieb, E. Rudolph, J. C. Steiner, R. R. Alfano, *Opt. Lett.* **2005**, *30*, 589.
[21] J. Le galudec, M. Dupoy, V. Rebuffel, P. Marcoux, *Biomed. Vib. Spectrosc* **2020**, p. 113590B.
[22] P. Y. Liu, L. K. Chin, W. Ser, T. C. Ayi, P. H. Yap, T. Bourouina,Y. Leprince-Wang, *Procedia Eng.* **2014**, *87*, 356.
[23] K. F. A. Ross, E. J. Billing, *Gen. Microbiol.* **1957**, *16*, 418.
[24] P. Y. Liu, L. K. Chin, W. Ser, T. C. Ayi, P. H. Yap, T. Bourouina,Y. Leprince-Wang, *Lab Chip* **2014**, *14*, 4237.
[25] P. J. Wyatt, *Nature* **1970**, *226*, 277.
[26] L.-H. Guillemot, M. Vrignaud, P. R. Marcoux, C. Rivron,T.-H. Tran-Thi, *Phys. Chem. Chem. Phys.* **2013**, *15*, 15840.
[27] H. C. Berg, *Phys. Today* **2000**, *53*, 24.
[28] R. J. Doyle, R. E. Marquis, *Trends Microbiol.* **1994**, *2*, 57.
[29] J. J. Thwaites, U. C. J. Suranat, *J. Bacteriol.* **1991**, *173*, 197.
[30] P. D. Skottrup, M. Nicolaisen, A. F. Justesen, *Biosens. Bioelectron.***2008**, *24*, 339.
[31] P. Arora, A. Sindhu, N. Dilbaghi, A. Chaudhury, *Biosens. Bioelectron.***2011**, *28*, 1.
[32] D. J. Dwyer, M. A. Kohanski, J. J. Collins, *Curr. Opin. Microbiol.* **2009**,*12*, 482.
[33] D. J. Dwyer, J. J. Collins, *Nat. Rev. Microbiol.* **2010**, *8*, 423.
[34] J. M. Wood, *Microbiol. Mol. Biol. Rev.* **1999**, *63*, 230.
[35] R. E. Marquis, *J. Bacteriol.* **1973**, *116*, 1273.
[36] K. Foubert, L. Lalouat, B. Cluzel, E. Picard, D. Peyrade,E. Delamadeleine, F. de Fornel, E. Hadji, *Appl. Phys. Lett.* **2008**, *93*, 251103.
[37] L. Lalouat, B. Cluzel, P. Velha, E. Picard, D. Peyrade, J. P. Hugonin,P. Lalanne, E. Hadji, F. de Fornel, *Phys. Rev. B* **2007**, *76*, 041102.
[38] C. Pin, B. Cluzel, C. Renaut, E. Picard, D. Peyrade, E. Hadji,F. de Fornel, *ACS Photonics* **2015**, *2*, 1410.
[39] C. Renaut, B. Cluzel, J. Dellinger, L. Lalouat, E. Picard, D. Peyrade, E. Hadji, F. de Fornel, *Sci. Rep.* **2013**, *3*, 2290.
[40] N. Descharmes, U. P. Dharanipathy, Z. Diao, M. Tonin, R. Houdré, *Lab Chip* **2013**, *13*, 3268.
[41] C. Pin, B. Cluzel, C. Renaut, D. Peyrade, E. Picard, E. Hadji,F. de Fornel, *Appl. Phys. Lett.* **2014**, *105*, 171108.
[42] K. S. Kunz, R. J. Luebbers, in *The Finite Difference Time Domain Method for Electromagnetics*, *CRC Press*, New-York, US **1993**,pp. 11–51.
[43] J. B. Bateman, J. Wagman, E. L. Carstensen, *Kolloid-Z. Polym.* **1966**,*208*, 44.
[44] T. J. Silhavy, D. Kahne, S. Walker, *Cold Spring Harbor Perspect. Biol.***2010**.
[45] J. M. Willey, L. M. Sherwood, C. J. Woolverton, *Prescott, Harley& Klein's Microbiology*, 7th ed., Mc Graw Hill, New York **2008**, p. 55.
[46] M. R. J. Salton, K.-S. Kim, in *Medical Microbiology*, 4th ed. (Ed:S. Baron), University of Texas Medical Branch, Galveston, US **1996**, p. 2.
[47] M. P. Doyle, J. L. Schoeni, *Appl. Environ. Microbiol.* **1984**, *48*, 855.
[48] Y. Yang, M. I. Kadim, W. J. Khoo, Q. Zheng, M. I. Setyawati,Y.-J. Shin, S.-C. Lee, H.-G. Yuk, *Int. J. Food Microbiol.* **2014**, *191*, 24.
[49] Y. Yang, W. J. Khoo, Q. Zheng, H.-J. Chung, H.-G. Yuk, *Int. J. Food Microbiol.* **2014**, *172*, 102.
[50] N. Haddaji, A. K. Mahdhi, B. Krifi, M. B. Ismail, A. Bakhrouf, *FEMS Microbiol. Lett.* **2015**, *362*, fnv047.
[51] R. Noor, *SpringerPlus* **2015**, *4*, 599.
[52] A. M. Wesche, J. B. Gurtler, B. P. Marks, E. T. Ryser, *J. Food Prot.* **2009**, *72*, 1121.
[53] A. Novelli-Rousseau, I. Espagnon, D. Filiputti, O. Gal, A. Douet, F. Mallard, Q. Josso, *Sci. Rep.* **2018**, *8*, 3957.
[54] C.-A. D. Burnham, R. A. Frobel, M. L. Herrera, B. L. Wickes, *J. Clin.Microbiol.* **2014**, *52*, 982.
[55] Z. Boz, R. Uyar, F. Erdoğdu, in *Encyclopedia of Food Microbiology*, Vol. *2*, 2nd ed. (Eds: C. A. Batt, M.-L. Tortorello), Academic Press,London, UK **2014**, pp. 160–168.

Figure 1.

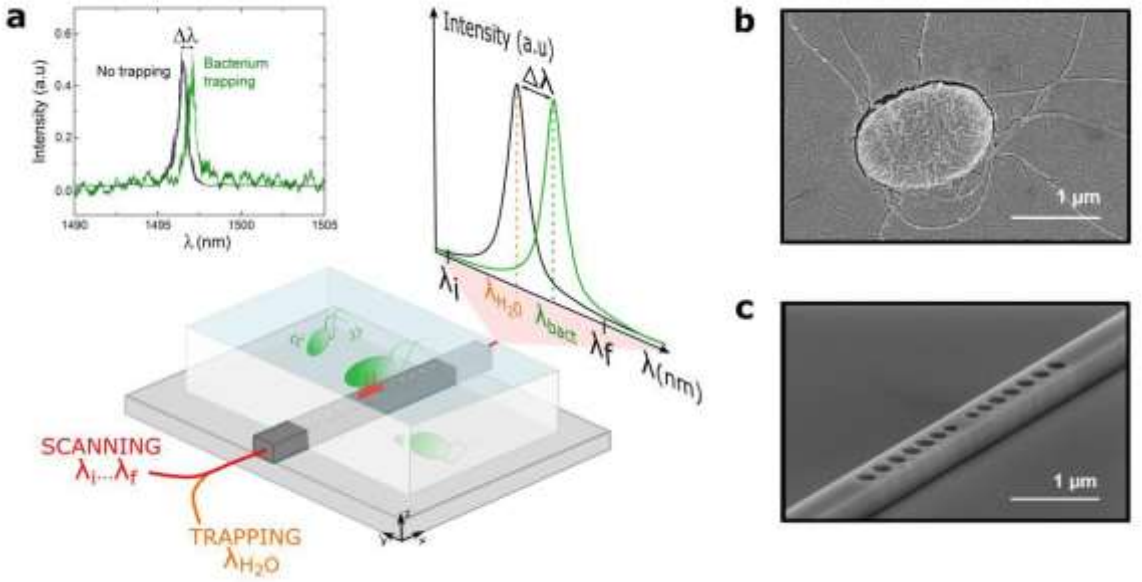

Figure 1. General principle, studied bacterium and optical micro-resonator. a) Experimental set-up developed to determine the microcavity resonant wavelength shift $\Delta\lambda$ ($\Delta\lambda = \lambda$bact $- \lambda$H O) caused by bacterial trapping. The inset presents experimental measurements of a resonant wavelength shift in the presence of a trapped bacterium. The intensity represented is the one transmitted by the optical structure (nanocavity). Oscillations in intensity (green curve) are due to the shift in the resonant wavelength during the displacement of the trapped bacterium in the evanescent field.[6] b) SEM image of the bacterium *E. coli*. c) SEM image of the micro-resonator designed specifically for *E. coli* trapping, that is, a 1D photonic crystal etched in a silicon ridge waveguide.

Figure 2.

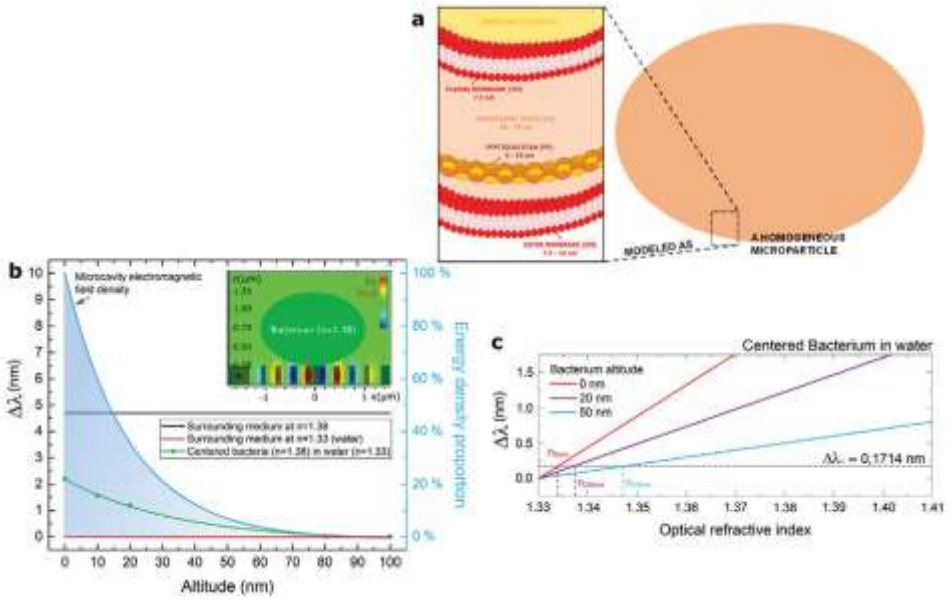

Figure 2. EMF interaction with the Gram-negative bacterial cell wall. a) Scheme of the multi-layered cell wall structure of a Gram-negative bacterium. For the FDTD simulations, the whole bacterial cell is modeled as a homogeneous rod-shaped microparticle, with constant dimensions. This very sim- plified framework yields an evaluation of the average RI of bacterial cell wall, within the evanescent field. b) Comparison of the resonant wavelength of a cavity surrounded by a medium with the same average RI as an *E. coli* cell $n = 1.38$ (black curve) and a medium of the index of water ($n = 1.33$) with that of a cavity with a trapped bacterium (modeled by a 1×2 μm rod shape) in aqueous medium (green curve). These results are shown in rela- tion to the resonant wavelength of the cavity in water ($\Delta\lambda = \lambda_{bact} - \lambda_{H\,O}$). The blue curve represents the EMF decline above the microcavity. The inset depicts the distribution of the EMF in the microresonator in the presence of a rod-shaped bacterium (zero-distance between bacterium and cavity). All these results are derived from FDTD calculations. c) Abacus plotting the resonance shift versus the RI of bacterial cell, for several bacterium altitude (microcavity-bacterium distance). It is constructed for a specific micro-resonator using FDTD calculation of the resonant wavelength during the trap- ping of a bacterium in water (normalization against the cavity resonant wavelength in water).

Figure 3.

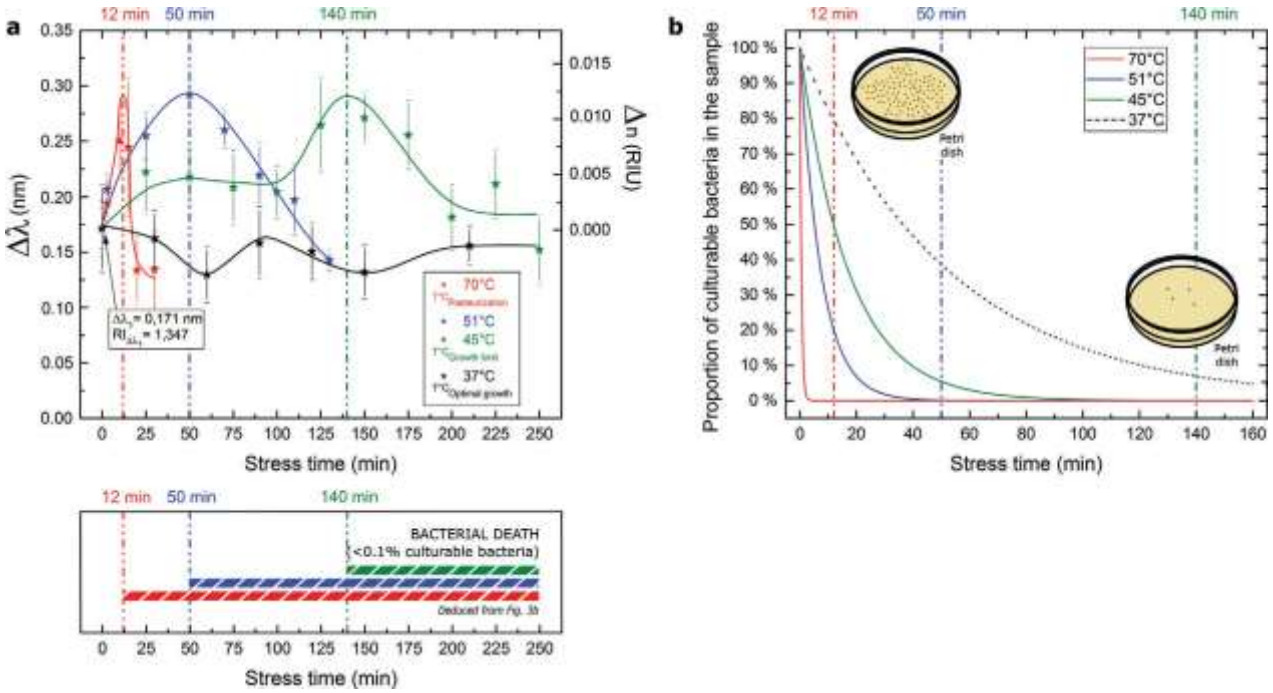

Figure 3. Effect of thermal stress on the surface RI of the trapped bacterial cell wall (i.e., the cell wall RI averaged within the evanescent field). a) Evolution of the average microcavity resonant wavelength shift $\Delta\lambda$ when bacteria are trapped, as a function of the heating time at 37, 45, 51, and 70 °C. The results are presented as mean value +/− standard deviation.[2] The evolution of the surface cell wall RI is calculated using the method previ- ously described, and assumes that the bacterium is located at 50 nm above from the optical cavity. The right axis corresponds to Δn, the shift of the trapped bacteria RI compared to a non-stressed bacterium. All measurements are normalized with respect to the mean value of resonant shift caused by non-stressed bacteria ($\Delta\lambda 1 = 0.171 \pm 0.043$ nm) and normalized against the resonant wavelength of the water-surrounded cavity ($\Delta\lambda = \lambda_{bact} - \lambda$H O). The proportion of culturable bacteria in the stressed sample is represented, deducted from the results shown in Figure 3b (see the Experimental Sec- tion for more details). b) Proportion of survivors (culturable bacteria) measured through culture-based methods (colony forming units CFU) versus the minutes of exposure to heating at 37, 45, 51, and 70 °C). The vertical lines represent the maximum of each of the curves in Figure 3a. The curves at 45, 51, and 70 °C are plotted using the measured values of the decimal reduction times D_x (see Experimental section). The curve at 37 °C appears dotted because it is deduced from the other three curves by the calculation of z-value.